# The membranotropic activity of N-terminal peptides from the pore-forming proteins sticholysin I and II is modulated by hydrophobic and electrostatic interactions as well as lipid composition

Uris Ros[1], Lohans Pedrera[1], Daylín Díaz[1], Juan C de Karam[1], Tatiane P Sudbrack[2], Pedro A Valiente[1], Diana Martínez[1], Eduardo M Cilli[3], Fabiola Pazos[1], Rosangela Itri[2], Maria E Lanio[1], Shirley Schreier[4] and Carlos Álvarez[1,*]

[1]*Center for Protein Studies, Biology Faculty, University of Havana, Havana, Cuba*

[2]*Department of Applied Physics, Institute of Physics, University of São Paulo, São Paulo, Brazil*

[3]*Department of Biochemistry, Institute of Chemistry, São Paulo State University, Araraquara, São Paulo, Brazil*

[4]*Department of Biochemistry, Institute of Chemistry, University of São Paulo, São Paulo, Brazil*

**Corresponding author (Fax, +53-832-12321; Email, calvarez@fbio.uh.cu)*

The sea anemone *Stichodactyla helianthus* produces two pore-forming proteins, sticholysins I and II (St I and St II). Despite their high identity (93%), these toxins exhibit differences in hemolytic activity that can be related to those found in their N-terminal. To clarify the contribution of the N-terminal amino acid residues to the activity of the toxins, we synthesized peptides spanning residues 1–31 of St I ($StI_{1-31}$) or 1–30 of St II ($StII_{1-30}$) and demonstrated that $StII_{1-30}$ promotes erythrocyte lysis to a higher extent than $StI_{1-31}$. For a better understanding of the molecular mechanism underlying the peptide activity, here we studied their binding to lipid monolayers and pemeabilizing activity in liposomes. For this, we examined the effect on peptide membranotropic activity of including phospatidic acid and cholesterol in a lipid mixture of phosphatidylcholine and sphingomyelin. The results suggest the importance of continuity of the 1–10 hydrophobic sequence in $StII_{1-30}$ for displaying higher binding and activity, in spite of both peptides' abilities to form pores in giant unilamellar vesicles. Thus, the different peptide membranotropic action is explained in terms of the differences in hydrophobic and electrostatic peptide properties as well as the enhancing role of membrane inhomogeneities.

[Ros U, Pedrera L, Díaz D, de Karam JC, Sudbrack TP, Valiente PA, Martínez D, Cilli EM, Pazos F, Itri R, Lanio ME, Schreier S and Álvarez C 2011 The membranotropic activity of N-terminal peptides from the pore-forming proteins sticholysin I and II is modulated by hydrophobic and electrostatic interactions as well as lipid composition. *J. Biosci.* **36** 781–791] **DOI** 10.1007/s12038-011-9156-4

## 1. Introduction

The pore-forming proteins sticholysin I and sticholysin II (St I/II) produced by the sea anemone *Stichodactyla helianthus* (Lanio *et al.* 2001) are highly hemolytic toxins with 93% sequence identity. St I and II form hydrophilic pores both in natural and model lipid membranes of around 1 nm hydrodynamic radius (Tejuca *et al.* 2001). Despite the extensive work carried out aiming at clarifying how these water-soluble proteins bind, oligomerize and eventually disrupt target membranes, the role of each amino acid sequences or domains involved in the

**Keywords.** Actinoporin; hemolytic peptide; permeabilizing activity; pore-forming toxin; sticholysin

Abbreviations used: μ, mean hydrophobic moment; π, surface pressure; CF, carboxyfluorescein; Chol, cholesterol; GUV, giant unilamellar vesicles; H, mean hydrophobicity; LUV, large unilamellar vesicle; MLV, multilamellar vesicles; PA, phosphatidic acid; PC, phosphatidyl choline; SM, sphingomyelin; St I and St II, sticholysins I and II

mechanism of lysis it is barely known (Tejuca *et al.* 1996; Martínez *et al.* 2001; Álvarez *et al.* 2009). Sticholysins belong to the actinoporin family, a unique class of eukaryotic pore-forming toxins exclusively found in sea anemones (Kem 1988). Actinoporins are cysteine-less proteins with molecular weight around 20 kDa and high affinity for sphingomyelin (SM)-containing membranes (Anderluh and Maček 2002).

The main difference in the primary sequence between sticholysins lies in their N-terminal, where all non-conservative substitutions and one conservative substitution are found (Huerta *et al.* 2001). Compared to St II, St I contains two additional anionic amino acid residues ($Glu^2$ and $Asp^9$) instead of non-polar amino acid Ala, in positions 1 and 8 of St II. St I has an extra polar residue (Ser) at position 1, rendering St II's N-terminal 1–10 sequence more hydrophobic than its counterpart in St I. The most noteworthy functional difference between these toxins is that the lytic activity of St II is approximately 3- to 6-fold higher than that of St I in human red blood cells (Martínez *et al.* 2001). Since the N-terminal region of sticholysins is probably involved in pore formation (Álvarez *et al.* 2003; Mancheño *et al.* 2003; Casallanovo *et al.* 2006), their different hemolytic activity could be due, at least partly, to differences in this region.

To gain insight into the molecular mechanism of the differential activity of sticholysins, two peptides reproducing the N-terminal sequence of St I comprising residues 1–31 ($StI_{1-31}$) or the equivalent segment in St II ($StII_{1-30}$) were synthesized (table 1). The fragments contain the amphipathic α-helix (14–23 in St II and 15–24 for St I) preceded by a more (St II) or less (St I) hydrophobic sequence described for sticholysins (Mancheño *et al.* 2003; Castrillo *et al.* 2009). St II peptide is cationic at pH 7 (net charge +2) in contrast to $StI_{1-31}$, which has no net charge. In a previous characterization of peptide activity, we demonstrated that $StII_{1-30}$ is 3-fold more active than $StI_{1-31}$, qualitatively reproducing the differential hemolytic activity of toxins, which suggests that the N-terminal plays a key role in protein function (Cilli *et al.* 2007).

Here, we compare peptide binding to lipid monolayers formed at the air–water interface and correlate them with their ability to permeabilize liposomes of different composition. To this end, interaction of peptides with membranes composed of phosphatidylcholine (PC) and SM, the anionic phospholipid phospatidic acid (PA) and cholesterol (Chol) were studied. Results obtained here were explained in terms of differences in the molecular mechanism of action modulated by dissimilarity in hydrophobic continuity of the sequence 1–10/11 and net charge between $StII_{1-30}$ and $StI_{1-31}$, respectively.

## 2. Materials and methods

### 2.1 *Chemicals and reagents*

All 9-fluorenylmethyloxycarbonyl amino acids and Rink-amide MBHAR resin were purchased from Advanced Chemtech (Louisville, KY, USA) and Novabiochem (San Diego, CA, USA). Egg phosphatidylcholine (PC), egg sphingomyelin (SM), 1-palmitoyl-2-oleoyl-sn-glycero-3-phosphate (PA) and cholesterol (Chol) were purchased from Avanti Polar Lipids (Alabaster, AL, USA), claimed to be 99% pure, and were used without further purification. Solvents and reagents were from Sigma–Aldrich Co (St Louis, MO, USA) and Fluka (Buch, Switzerland).

### 2.2 *Peptide synthesis*

The peptides, with amidated C-terminus, were synthesized manually according to the standard $N_\alpha$-Fmoc protecting-group strategy (Atherton and Sheppard 1988) as previously described (Casallanovo *et al.* 2006). The peptides' homogeneity was checked by analytical HPLC (Varian, Walnut

**Table 1.** Peptide sequences, net charge, average hydrophobicity (H) and mean hydrophobic moment (μ)

| Peptide | Sequence | Net Charge (pH 7) | H | | μ | | Predicted orientation | |
|---|---|---|---|---|---|---|---|---|
| | | | 1–11* | 14–24* | 1–11* | 14–24* | 1–11* | 14–24* |
| $StI_{1-31}$ | SELAGTIIDGASLTFEVLDKVLGELGKVSRK-$NH_2$ | 0 | 0.38 | 0.28 | 0.41 | 0.55 | Surface | Surface |
| $StII_{1-30}$ | ALAGTIIAGASLTFQVLDKVLEELGKVSRK-$NH_2$ | +2 | 0.64 | 0.16 | 0.16 | 0.66 | Transmembrane | Surface |

The differences between sticholysins's peptides are underlined. All peptide C-terminal are amidated.

*The sequences include the hydrophobic stretch 1–11 and the amphiphilic α-helix 14–24 according to the 3D structure of St II (Mancheño *et al.* 2003) or 1–11 and 15–25 according to 3D structure of St I (Castrillo *et al.* 2009). H and μ were calculated according to the Eisenberg procedure (Eisenberg *et al.* 1984). This method uses an optimized 11-residue window and an angular frequency between consecutive residues fixed at 100° (program *MOMENT Transmembrane Helix Prediction*, http://www.doe-mbi.ucla.edu/services).

Creek, CA, USA), using UV detection at 220 nm. The identity of the peptides was confirmed by electrospray mass spectrometry on a ZMD model apparatus (Micromass, Manchester, UK) and amino acid analysis (Shimadzu, Tokyo, Japan).

### 2.3 *Surface pressure measurements on lipid monolayers*

Surface pressure measurements were carried out with a μThrough-S system (Kibron, Helsinki, Finland) at 25°C under constant stirring employing plates of ca. 3.14 $cm^2$. The aqueous phase consisted of 300 μL of Tris-buffered saline (TBS: 145 mM NaCl, 10 mM Tris–HCl, pH 7). The lipidic mixture pre-dissolved in chloroform:methanol (2:1, v:v) was gently spread over the surface, and the desired initial surface pressure ($\pi_0$) was attained by changing the amount of lipid applied to the air–water interface. The peptides were injected into the sub-phase to achieve 0.1 μM peptide final concentration, at which peptides have no effect on surface tension of the air–water interface. The increment in surface pressure ($\Delta\pi$) was recorded as a function of the elapsed time until a stable signal was obtained.

### 2.4 *Leakage studies from carboxyfluorescein containing-LUV*

Large unilamellar vesicles (LUV) were prepared by extruding a solution of multilamellar vesicles (MLV) in the presence of 80 mM carboxyfluorescein (CF) (pH 7 adjusted by adding NaOH), and subjected to six cycles of freezing and thawing. A two-syringe LiposoFast Basic unit extruder (Avestin Inc., Ontario, Canada) was used, equipped with two stacked 100 nm polycarbonate filters (Nuclepore, Maidstone, UK). To remove untrapped fluorophore, vesicles were filtered through a mini-column (Pierce, Rockford, USA) loaded with Sephadex G-50-medium pre-equilibrated with TBS. LUV permeabilization was determined using a FLUOstar OPTIMA microplate reader (BMG Labtech, Offenburg, Germany) by measuring the fluorescence ($\lambda_{exc}$=490 nm and $\lambda_{em}$=520 nm) of released CF. Black plastic 96-well microplates (SPL-Life Sciences, Seoul, South Korea) were pretreated with 0.1 mg/mL Prionex (Pentapharm, Basel, Switzerland), which strongly reduces unspecific binding of protein and vesicles to plastic (Dalla Serra *et al.* 1999). Each well was filled with the elution buffer plus 10 μM of LUV. Finally, peptide was added, in a total volume of 200 μL, at the final concentration reported in the text. After mixing vesicles and peptides, the release of CF produced an increase in fluorescence (*f*), due to the dequenching of the dye into the external medium, which was resolved in time. Spontaneous leakage of dye was negligible under these conditions. Maximum release was always obtained by adding 1 mM Tx100 (final concentration) and provided the fluorescence value $f_{max}$. The fraction of fluorophore release (*F*) was calculated as follows:

$$F = (ft - fo)/(f_{max} - fo) \quad (1)$$

where *fo* and *ft* represent the value of fluorescence before or at time *t* after peptide addition, respectively.

Phospholipid concentration was mesuared by determining inorganic phosphate according to Rouser *et al.* (1970).

### 2.5 *Optical microscopy of giant unilamellar vesicles*

Giant unilamellar vesicles (GUV) were grown using the electroformation method (Angelova and Dimitrov 1986). Briefly, 16 μL of a 2 mg/mL lipid in chloroform solution were spread on the surfaces of two conductive glasses coated with Fluor Tin Oxide, which were then placed with their conductive sides facing each other and separated by a 2 mm thick Teflon frame. This electroswelling chamber was filled with 0.2 M sucrose solution and connected to an alternating current of 1 V with a 10 Hz frequency for 2 h. The vesicle suspension was removed from the chamber and diluted ~10 times into a 0.2 M glucose solution containing 10–80 nM of peptide. The osmolarities of the sucrose and glucose solutions were previously measured with a Gonotec 030 cryoscopic osmometer (Osmomat, Berlin, Germany) and carefully matched to avoid osmotic pressure effects. Then, vesicles were immediately placed in the observation chamber. Due to the differences in density and refractive index between sucrose and glucose solutions, the vesicles were stabilized by gravity at the bottom of the observation chamber and visualized with a 63x Ph2 objective in phase contrast mode of an inverted microscope Zeiss Axiovert 200 (Zeiss, Jena Germany) equipped with a Zeiss AxioCam digital camera (Zeiss, Jena, Germany).

## 3. Results

### 3.1 *Hydrophobic and amphipatic properties of $StI_{1-31}$ and $StII_{1-30}$*

A distinctive feature of $StII_{1-30}$ when compared with $StI_{1-31}$ is the higher mean hydropathy index of its first 10 N-terminal residues (figure 1A). In addition, sequences comprising residues 14–31 ($StI_{1-31}$) and 13–30 ($StII_{1-30}$) are characterized by a high mean hydrophobic moment (μ) (figure 1B), as indicator of the amphiphilicity of an α-helix (Eisenberg *et al.* 1984). Both properties, the presence of a highly hydrophobic sequence followed by an amphipatic α-helix, are representative characteristics of membrane spanning pore-forming peptides. While the hydrophobic stretch may help to partition into membrane hydrophobic core, the

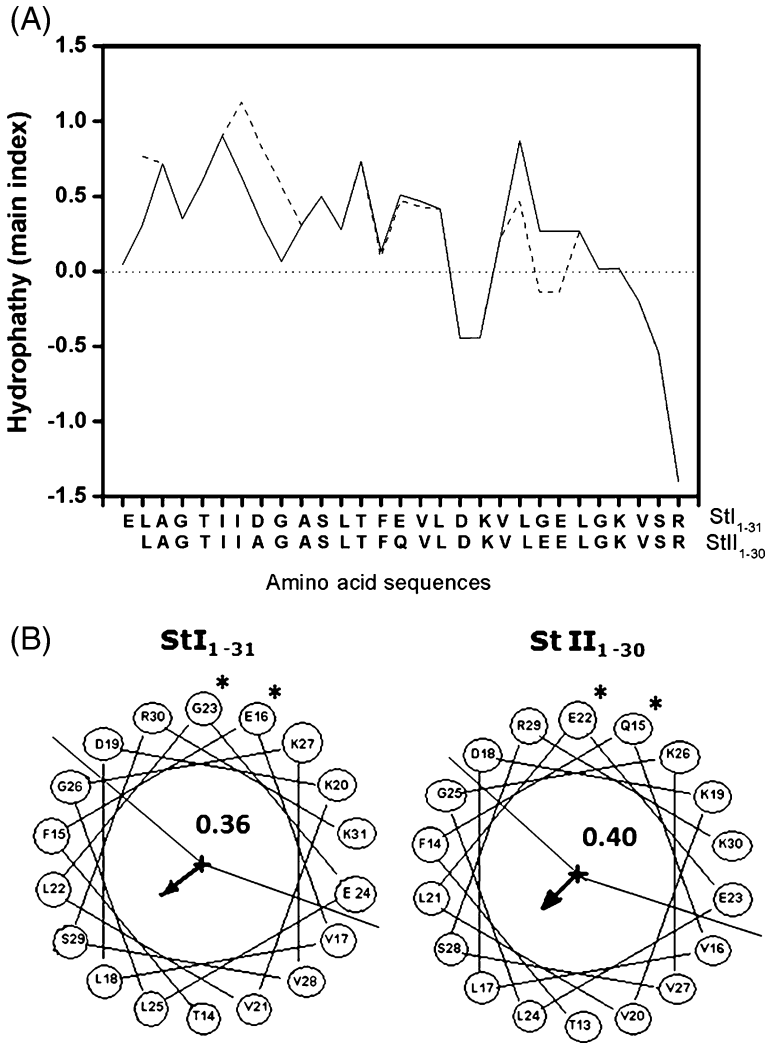


**Figure 1.** $StI_{1-31}$ and $StII_{1-30}$ hydrophathy profiles and wheel projections of their amphiphilic segments. (**A**) Hydrophathy profile $StI_{1-31}$(–) and $StII_{1-30}$ (- -). Calculations were based on the hydropathy values reported by Eisenberg (Eisenberg *et al.* 1984). (**B**) Wheel projections with their corresponding μ of the most amphiphilic segment of $StI_{1-31}$ (14–31) and $StII_{1-30}$ (13–30). Differences between $StI_{1-31}$ and $StII_{1-30}$ sequences are labeled with asterisks. The μ is indicated by an arrow that points towards the hydrophobic face of the helix (Eisenberg *et al.* 1984).

amphipatic helix would contribute to form the hydrophilic pore (Yeaman and Yount 2003).

The Hydrophobic Moment Plot is often used to identify putative transmembrane α-helices of integral membrane proteins, based on the relation between their μ and the corresponding mean hydrophobicity (H). The resulting plot classifies the peptides according to their propensity to be a putative transmembrane peptide or a surface seeking one (Eisenberg *et al.* 1984). Table 1 shows H and μ calculated for 1–11 and the 14–24/15–25 sequences from $StII_{1-30}$/$StI_{1-31}$, respectively. The major difference between these peptides is given by the higher H and lower μ of the 1–11 amino acid segment of $StII_{1-30}$ in contrast to $StI_{1-31}$. In fact, taking into account these parameters, this sequence is predicted as a transmembrane segment in $StII_{1-30}$, while in $StI_{1-31}$ the equivalent stretch is predicted as a surface seeking one. Regarding the segment that includes the α-helix of sticholysins, it was predicted as a surface seeking for both peptides due to their higher μ and lower H.

### 3.2 *Binding to lipid monolayers*

The increase in surface pressure by the association of peptides to previously formed lipid monolayers at the air–water interface can be employed to characterize their ability to interact with organized lipids. To this end, the studied lipid monolayers were composed of PC:SM (50:50),

PC:SM:PA (50:45:5), PC:SM:Chol (20:45:35) and PC:SM:PA:Chol (30:45:5:20). PC:SM was selected as a starting mixture since this binary composition has proved to be adequate for binding of sticholysins to lipid membranes (Tejuca *et al.* 1996). Chol is a more apolar structure than the other lipids studied and was incorporated into a mixture of PC and SM due to its abundance and regulatory properties in membranes (Sackmann 1995); in fact, Chol and SM tend to form microdomains in membranes (Simons and Vaz 2004). Finally, inclusion of the anionic phospolipid PA allowed studying the influence of electrostatic interactions on peptide binding. This phospholipid is present only in small amount in the outer layer of the citoplasmatic membrane (Op dem Kamp 1979; Langner and Kubica 1999), thus including 5 mole% into the lipid mixture could be mimicking the cell composition of mammalian cells.

The increase in surface pressure ($\Delta\pi$) due to peptide interaction was evaluated at several initial pressures ($\pi_0$) of the lipid monolayer. Figure 2 shows $\Delta\pi$ at equilibrium upon $StI_{1\text{-}31}$ (figure 2A) or $StII_{1\text{-}30}$ (figure 2B) addition as a function of $\pi_0$ for monolayers of different compositions. A suitable parameter for the characterization of peptide–lipid interaction is the critical pressure ($\pi_c$), obtained by extrapolating to zero the $\Delta\pi$ at equilibrium as a function of $\pi_0$ (insets, figures 2 A and B). This parameter corresponds to the minimum pressure that must be applied to avoid incorporation of the peptide into a monolayer and is directly correlated with its affinity for the monolayer (Brockman 1999).

In zwitterionic PC:SM (50:50) monolayers (figure 2) $\pi_c$ for $StII_{1\text{-}30}$ was higher than that for $StI_{1\text{-}31}$. In fact $\pi_c$ for $StII_{1\text{-}30}$ is close to 35 mN $m^{-1}$, which corresponds to the lateral pressure of a typical biological membrane (Brockman 1999). Even though such surface pressure is only an average value that can undergo large fluctuations depending on its compressibility (Phillips *et al.* 1975), it has been proposed that when $\pi_c$ is higher than this critical limit, the peptide not only associates to the monolayer but also penetrates it (Caaveiro *et al.* 2001).

The inclusion of PA in the PC:SM mixture, promoted an increase in $\pi_c$ for $StII_{1\text{-}30}$ but no change was observed for $StI_{1\text{-}31}$. In PC:SM monolayers, the difference between both peptides in terms of $\pi_c$ is around 4.77 mN $m^{-1}$, being even higher in PC:SM:PA (7.71 mN $m^{-1}$). The fact that PA-enhanced binding differences by promoting a larger interaction of $StII_{1\text{-}30}$ to this negatively charged monolayer points out a possible role of peptides' charge on their binding to membranes. In order to further understand the involvement of the two negatively charged residues ($Glu^2$ and $Asp^9$) of $StI_{1\text{-}31}$, not present in $StII_{1\text{-}30}$ (table 1) for binding, we also synthesized a shorter peptide, $StI_{12\text{-}31}$, which lacks these two anionic residues and assessed its interaction with PC:SM:PA monolayer. This shorter peptide is characterized by a positive charge of +2 at pH 7, keeping the charged residues situated in the amphiphilic portion of $StI_{1\text{-}31}$ (table 1). When $StI_{1\text{-}31}$ was devoid of the first N-terminal 11 amino acids, the truncated peptide, i.e. $StI_{12\text{-}31}$, yielded a higher $\pi_c$ in the negatively charged monolayer ($\pi_c$=30.10 mN $m^{-1}$). These results clearly indicate that the first sequence of St I carrying the two extra anionic residues ($Glu^2$ and $Asp^9$) somehow hinders binding to the negatively charged membrane.

Incorporation of Chol into the starting lipid ensemble (PC:SM) did not modify binding of $StI_{1\text{-}31}$ when compared to the monolayer devoid of this sterol (figure 2A), in contrast with $StII_{1\text{-}30}$, which showed an increase in the affinity for the Chol-containing monolayer (figure 2B). Similar to the increase promoted by PA, Chol enhanced the difference of $\pi_c$ between both peptides from 4.77 mN $m^{-1}$ in PC:SM monolayer to 7.1 mN $m^{-1}$ in PC:SM:Chol monolayer. To clarify if the preferential binding of $StII_{1\text{-}30}$ to this monolayer – in which the hydrophobic properties were enhanced due to Chol – was related to the presence of the higher hydrophobic segment 1–10, a shorter peptide $StII_{11\text{-}30}$ was also synthesized. This peptide lacks the first 10 amino acids of $StII_{1\text{-}30}$ but keeps peptide charge (+2 at pH 7) since it shares the same ionizable groups. The deletion of 1–10 sequence of $StII_{1\text{-}30}$ elicited a decrease in the affinity for the monolayer evidenced in a lower $\pi_c$ value of $StII_{11\text{-}30}$ (31.89 mN $m^{-1}$) compared to $StII_{1\text{-}30}$ (figure 2B). Altogether the results point out that affinity of $StI_{1\text{-}31}$ or $StII_{1\text{-}30}$ for a lipid monolayer is mainly influenced by the first ten or eleven amino acid residues of their N-terminal sequence.

In addition we studied binding of $StI_{1\text{-}31}$ and $StII_{1\text{-}30}$ to more complex monolayers of PC:SM:PA:Chol in an attempt to approach the lipid heterogeneity of erythrocyte membrane, a classical model target for studying the actinoporins' activity (Martínez *et al.* 2001) and their peptides (Cilli *et al.* 2007). It is remarkable that both peptides attain $\pi_c$ values higher than 35 mN $m^{-1}$ (figure 2 A and B), indicating that they probably penetrate this lipid monolayer (Caaveiro *et al.* 2001). In summary, this was the only monolayer to which $StI_{1\text{-}31}$ showed a relevant interaction. In fact, the differences in terms of $\pi_c$ between peptides diminished to 5.84 mN $m^{-1}$, as compared to monolayers containing either PA (7.71 mN $m^{-1}$) or Chol (7.10 mN $m^{-1}$), being higher than that found for PC:SM monolayer (4.77 mN $m^{-1}$) (inset, figures 2 A and B).

### 3.3 *Vesicles permeabilization by peptides*

Since the functional activity of peptides in terms of hemolysis (Cilli *et al.* 2007) and size of the pore formed by $StII_{1\text{-}30}$ (Casallanovo *et al.* 2006) have been previously characterized, in this study we examined whether $StI_{1\text{-}31}$ and $StII_{1\text{-}30}$ were able to permeabilize LUV of the same lipid compositions used in monolayer studies. Under the experimental

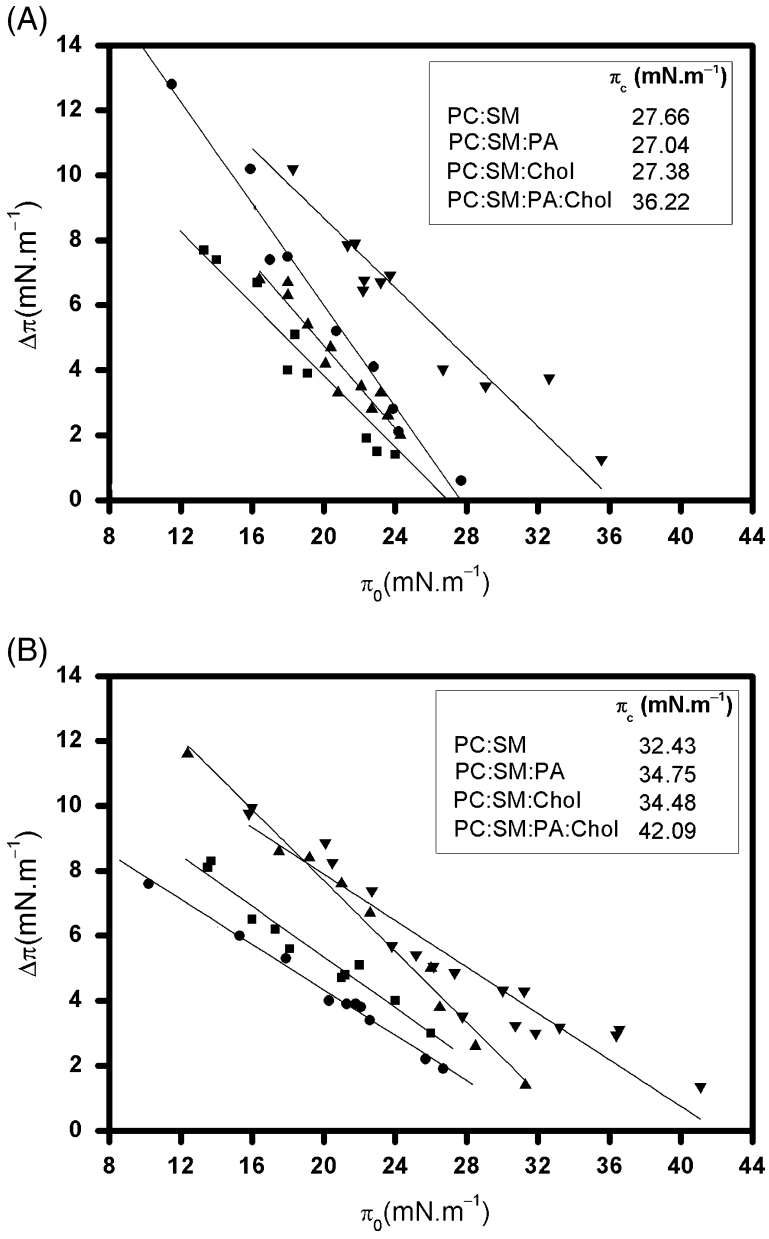


**Figure 2.** Critical pressure induced by peptides on monolayers of different lipid composition. (**A**) $StI_{1-31}$ and (**B**) $StII_{1-30}$. Critical pressure ($\pi_c$): Pressure that must be applied to avoid incorporation of the peptide into the monolayer, directly correlated with the affinity of the peptides for the lipids. $\Delta\pi$ is the pressure increase in the lipidic monolayer due to peptide binding. Lines represent the best linear fit of the $\Delta\pi$ as a function of the initial monolayer pressure ($\pi_o$). Peptide concentration: 0.1 μM. Buffer solution TBS pH 7. T~25°C. Lipid composition: PC:SM (50:50) (●), PC:SM:PA (50:45:5) (■), PC:SM:Chol (20:45:35) (▲), PC:SM:PA:Chol (30:45:5:15) (▼).

conditions employed herein, the phase behaviour of monolayer and liposomes has been reported to be the same (Veatch and Keller 2002).

Figure 3A exemplifies the time course of the CF release upon $StII_{1-30}$ addition to PC:SM LUV. This result evidences that both the initial rate as well as the extent of the process are time and dose dependent. The final extent of the fluorophore release elicited by the peptide (*F*) was plotted as a function of peptide concentration. In LUV, $StII_{1-30}$ promoted the release of the dye from the vesicles to a larger extent than $StI_{1-31}$ and its effect was dependent on peptide concentration (figures 3B–D). Similar to lipid binding, permeabilization activity is driven by interplay between peptide and membrane properties. The inclusion of PA enhanced $StII_{1-30}$ activity while that of $StI_{1-31}$ experienced a drastic fall remaining non-detectable. However, inclusion of

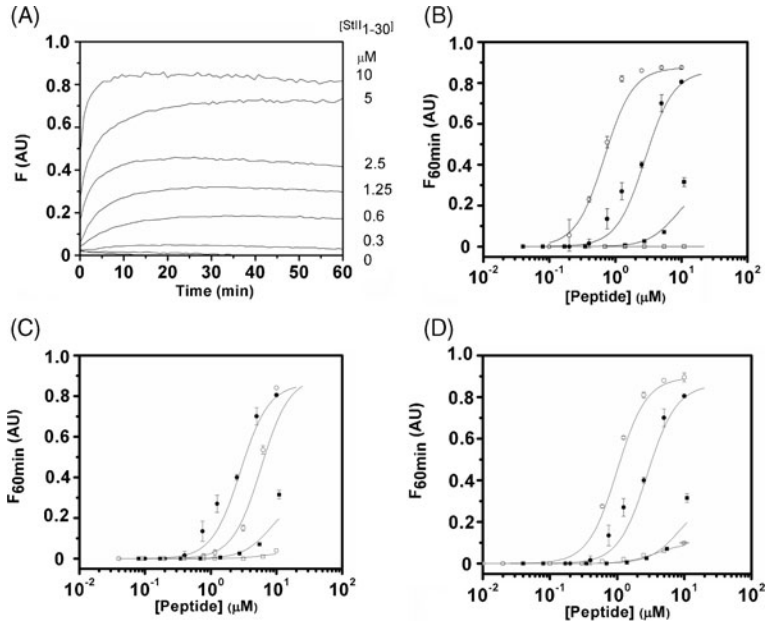


**Figure 3.** Release of carboxyfluorescein from LUV promoted by peptides. (**A**) Time course of PC:SM (50:50) LUV permeabilization as a function of $StII_{1-30}$ concentration. (**B**) Effect of PA on LUV permeabilization by peptides. (□) $StI_{1-31}$ with PC:SM:PA (50:45:5) LUV, (○) $StII_{1-30}$ with PC:SM:PA (50:45:5) LUV. (**C**) Effect of Chol on LUV permeabilization by peptides. (□) $StI_{1-31}$ with PC:SM:Chol (20:45:35) LUV, (○) $StII_{1-30}$ with PC:SM:Chol (20:45:35) LUV. **D**) Permeabilization of LUV composed by the quaternary mixture. (□) $StI_{1-31}$ with PC:SM:PA:Chol (30:45:5:20) LUV, (○) $StII_{1-30}$ with PC:SM:PA:Chol (30:45:5:20) LUV. For B, C and D (■) $StI_{1-31}$ with PC:SM (50:50) LUV, (●) $StII_{1-30}$ with PC:SM (50:50) LUV. *F*: fraction of fluorophore release. Curves in B, C and D were fitted to a Hill function ($F_{60min}=F_{max}$ [peptide]$^n$ / $C_{50}{}^n$+[peptide]$^n$) using Origin 8.0, Microcal Inc. (USA). Experiments were done in triplicate ($R^2>0.99$ and $\chi_{red}{}^2<10^{-4}$). Lipid concentration: 10 μM. Buffer solution TBS pH 7. T~25°C.

Chol into the lipid mixture dropped the permeabilizing activity of $StII_{1-30}$ and practically rendered $StI_{1-31}$ unable to permeabilize LUV (figure 3C). In the complex lipid mixture PC:SM:PA:Chol, $StII_{1-30}$ also showed a higher activity than $StI_{1-31}$ (figure 3D).

In order to compare the relative activity of $StII_{1-30}$ in presence of LUV of different compositions, permeabilization parameters were determined by fitting the experimental data to a Hill sigmoid model as showed in figures 3B, C and D. $F_{max}$ is the maximum dye release achieved at high peptide concentrations, while $C_{50}$ is the concentration necessary to promote the release of 50% of CF entrapped and *n* is the power dependence of *F* on toxin dose, the so-called cooperativity number (table 2). According to $F_{max}$, both peptides achieved their maximum activity in PC:SM liposomes promoting the permeabilization of c.a. 90% of vesicle ensemble in the assay. The fact that not all the vesicles were apparently permeabilized might be due to the fact that Triton X-100 affects the fluorescence of CF either directly (Chen and Knutson 1988) or indirectly, diminishing light scattering by disruption of membrane integrity. In addition, *n* was higher than 1 for all lipid compositions, indicating the necessity of a minimum number of peptide molecules for $StII_{1-30}$ permeabilization activity as described for actinoporins (Belmonte *et al.* 1993; Tejuca *et al.* 1996). Even though $F_{max}$ and *n* did not considerably differ among liposomal compositions, $C_{50}$ reflected the different $StII_{1-30}$ activity for all the lipid mixtures analysed. Liposomes containing PA (PC:SM:PA and PC:SM:PA:Chol) became around 3-fold more susceptible to permeabilization than PC:SM vesicles, in contrast to PC:SM:Chol in which the inclusion of Chol caused a drop of twice of the activity in PC:SM.

### 3.4 *Visualization of peptides effect on GUV*

With an aim to visualize the effect of both peptides on vesicles, GUV were diluted into peptide-containing glucose solution and immediately placed in the observation chamber. Changes in GUV features were followed over time by video microscopy. Figure 4 shows how the presence of 10 nM of $StII_{1-30}$ in the outer GUV solution impacted on PC:SM:PA:Chol lipid membrane that exhibited initially optical contrast due to sucrose/glucose asymmetry (snapshot A). Such a contrast gradually diminished with time, reflecting changes in the bilayer permeability as a result of the inner

**Table 2.** Parameters derived from LUV permeabilization induced by the peptides

| LUV composition | $StII_{1-30}$ | | |
|---|---|---|---|
| | $F_{max}$ | $C_{50}$ (μM) | $n$ |
| PC:SM (50:50) | 0.91±0.04 | 2.4±0.3 | 1.5±0.2 |
| PC:SM:PA (50:45:5) | 0.88±0.02 | 0.6±0 | 2.7±0.4 |
| PC:SM:Chol (20:45:35) | 0.91±0.01 | 5.5±0.1 | 2.9±0.1 |
| PC:SM:PA:Chol (30:45:5:20) | 0.89±0.02 | 0.9±0.1 | 2.4±0.3 |

$F_{max}$: maximum fluorescence attained at high peptide concentration, $C_{50}$: peptide concentration necessary to achieve 50% of $F_{max}$, $n$: cooperativity number derived from the power dependence of the fraction of fluorophore release ($F$) on toxin concentration. When $n$ results higher than 1 indicates cooperativity, i.e. suggests oligomerization even though cannot provide the true molecularity of the assembly for permeabilization.

All parameters were calculated by fitting dose-dependence curves of permeabilization induced by peptides (figures 3B, C and D) to a Hill sigmoid ($F_{60min}=F_{max}$ [peptide]$^n$ / $C_{50}{}^n$ +[peptide]$^n$ ) using Origin 8.0, Microcal Inc. (USA). Experiments were done in triplicate ($R^2 >$ 0.99 and $\chi_{red}{}^2 < 10^{-4}$ ).

and outer solutions exchange. The complete loss of membrane contrast was observed (snapshots B and C) within a time interval of 2 min of GUV visualization, without any change in the membrane integrity in terms of lipid bilayer solubilization and/or macropores opening. In fact, the increase in membrane permeability must be due to the formation of pores that are smaller than the microscope resolution of few microns. It is noteworthy that the GUV remained unchangeable up to 10 min of further continuous observation (snapshot none shown), implying that $StII_{1-30}$ promoted stable sub-micron pore formation in the lipid membrane. Similar observations were also recorded for $StI_{1-31}$ in contact with GUV of PC:SM:PA:Chol. Despite this similarity, 8-fold more molecules of $StI_{1-31}$ were required in comparison to $StII_{1-30}$ for visualizing the equivalent effect, which qualitatively correlated with binding to lipid monolayer and permeabilizing activity in LUV.

## 4. Discussion

St I and St II are characterized by a few amino acid substitutions spread throughout the primary sequence, exhibiting all the non-conservative changes in their N-terminal (Huerta *et al.* 2001). The presence of hydrophobic (≈ residues 1–10) and highly amphipathic (≈ residues 14–35) sequences in both St's N-terminal supports the assumption that this region is probably involved in pore formation (Anderluh and Maček 2002; Malovrh *et al.* 2003; Mancheño *et al.* 2003; Casallanovo *et al.* 2006; Álvarez *et al.* 2009; Castrillo *et al.* 2009). Both toxins exert their hemolytic action in human red blood cells in the nanomolar concentration range, but St II is about 5- to 6-fold more active than St I (Martínez *et al.* 2001). We have previously demonstrated by CD spectroscopy studies and theoretical predictions that the synthetic peptide $StII_{1-30}$ can mimic folding and functional properties of St II's N-terminus (Casallanovo *et al.* 2006). In that work we emphasized the contribution of St II's N-terminal region, in particular, the hydrophobic amino acid sequence 1–10 to pore formation. On the other hand, differences in activity observed between sticholysins were found to be correlated with the activity of $StI_{1-31}$ and $StII_{1-30}$ (Cilli *et al.* 2007). In addition, both peptides show a high propensity to acquire α-helical structure in trifluoroethanol, a well-known inducer of secondary structure (Buck 1998) and in liposomes, somehow reproducing the presence of an N-terminal α-helix of sticholysins (Mancheño *et al.* 2003; Castrillo *et al.* 2009).

In this work the relative influence of the hydrophobic and electrostatic interactions on peptides binding to lipid monolayers and permeabilizating activity in vesicles were analysed given that an adequate balance between the net charge and hydrophobicity is essential for membranotropic peptides to display their activity (Blondelle *et al.* 1999; Tossi *et al.* 2000; Yeaman and Yount 2003). To this end, experiments modulating membrane properties such as surface charge by including the anionic PA or membrane hydrophobicity and lipid organization by Chol addition to the basal PC:SM lipid mixture were performed.

A distinctive feature of $StII_{1-30}$ is the higher net positive charge (+2 at pH 7) (table 1) and larger mean hydropathy index of its first 10 N-terminal residues when compared to $StI_{1-31}$ (table 1 and figure 1). In contrast, $StI_{1-31}$ has no net charge at pH 7 on account of two additional acidic aminoacids ($Glu^2$ and $Asp^9$) in the hydrophobic segment 1–10 (table 1), which leads to a decrease in the hydrophobicity of this sequence. These attributes of peptide sequences may determine their different penetration upon binding to membranes as predicted (table 1). In fact, the lower $\pi_c$ showed by $StI_{1-31}$ (figure 2A) when compared to $StII_{1-30}$ in lipid monolayers (figure 2B) could reflect a less deep insertion into the membrane of the former peptide.

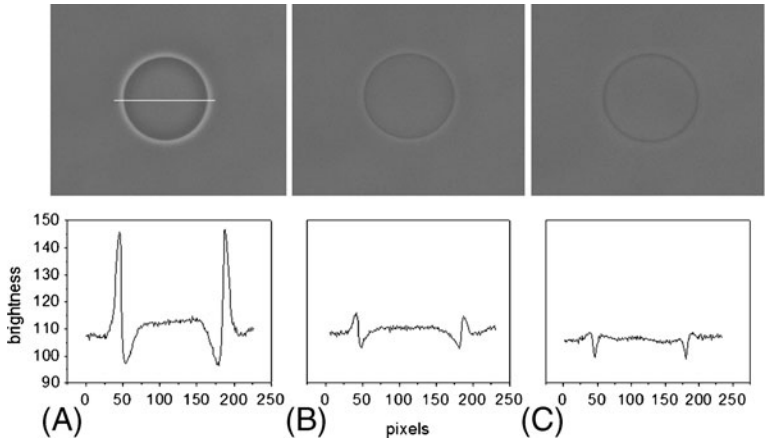


**Figure 4.** Visualization of the effect elicited by $StII_{1-30}$ on GUV. *Upper row*: GUV snapshots immediately placed in contact with $StII_{1-30}$ (**A**). GUV after 2 min (**B**) or 4 min (**C**) of visualization. *Lower row*: Line profile of the phase contrast. The solid line (in upper A) indicates the transversal section selected for the profiles. GUV composition PC:SM:PA:Chol (30:45:5:20). Internal solution 0.2 M sucrose, external solution 0.2 M glucose containing 10 nM of $StII_{1-30}$. T~25°C. $StI_{1-31}$ peptide impacted on membrane properties in a similar way, leading to a gradual loss of inner–outer medium contrast of the membrane with time, as shown as example in the figure for $StII_{1-30}$. Despite this similarity, 8-fold more molecules of $StI_{1-31}$ were required in comparison to $StII_{1-30}$ for visualizing the equivalent effect. After contrast loss, GUV remained unchangeable up to 1 hour on further continuous observation.

$StII_{1-30}$ shows not only a higher affinity for monolayers (insets figure 2A and B) but a larger vesicle permeabilization of membranes (figures 3 and 4) than its counterpart $StI_{1-31}$, in agreement with the previously informed relative hemolytic activity of these peptides (Cilli *et al.* 2007). In response to the peptides' net electric charge (table 1), modification of the surface membrane charge prompted different binding and permeabilizing activity of $StII_{1-30}$ and $StI_{1-31}$ (figures 2 and 3, respectively). The negatively charged membrane surface moderately increased the ability of the cationic $StII_{1-30}$ for binding to monolayers (figure 2B) and significantly enhanced its permeabilizing activity (figure 3 and table 2), suggesting the contribution of the electrostatic forces in vesicles permeabilization by this peptide. Conversely, the negatively charged surface membrane did not modify the low binding ability of the neutral $StI_{1-31}$ to zwitterionic membranes (figure 2) probably due to the presence of two anionic amino acidic residues ($Glu^2$ and $Asp^9$). These results clearly indicate the leader condition of the first 1–10 sequence for peptide binding and the essentiality of a hydrophobic continuum for a larger membrane perturbation. In spite of the fact that a lower affinity for $StI_{1-31}$ was not apparent for lipid monolayers (figure 2A), its activity decreased when PA was included in vesicles (figure 3B and table 2), suggesting that $Ser^1$, $Glu^2$ and $Asp^9$ may somehow impair membrane penetration or peptide oligomerization in this membrane model system.

Together with PC and SM, Chol is one of the most important lipids in eukaryotic cells, ranging up to 50 mole% in red blood cells (Sackmann 1995). There is evidence that high Chol concentration (> 35 mole%) in conjunction with sphyngolipids is vital to the formation of highly ordered lipid domains in membranes. As for St II and equinatoxin II – another actinoporin isolated from the Mediterranean Sea anemone *Actinia equina*, the presence of lipidic microdomains seems to provide a particularly favorable arrangement of lipids for the association and activity of these toxins with membranes (Barlič *et al.* 2004; Martínez *et al.* 2007). It has been also demonstrated that lateral heterogeneity of membrane favours the action of lytic peptides (Pokorny and Almeida 2005).

Taking into account the relevance of lipid microdomains for actinoporins and several membranotropic peptides, here we evaluated the effect of including Chol on peptides activity by comparing their action in PC:SM and PC:SM:Chol systems. Inclusion of Chol in a PC:SM monolayer promotes a moderate increase in binding of $StII_{1-30}$ (figure 2B) probably favoured by its 1–10 hydrophobic amino acid sequence. As expected for the lower hydrophobicity of the first 1–11 amino acid sequence of $StI_{1-31}$ (table 1), inclusion of Chol did not modify peptide binding to the lipid monolayer (figure 2A). Interestingly, inclusion of this lipid in liposomes containing PC:SM noticeably impairs the ability of both peptides for pore formation (figure 3C and table 2). A plausible explanation for the apparent contradiction as for $StII_{1-30}$ might be that membranes containing PC:SM:Chol do not favour the competent penetration and/or oligomerization of peptide for pore formation.

Moreover, here it was demonstrated the enhancing role of membrane lateral heterogeneity in peptide binding and activity. The notorious increase observed in binding for

both peptides to quaternary lipid monolayers supports this hypothesis (figures 2A and B). Nonetheless, $StII_{1-30}$ remained more active than $StI_{1-31}$ in both monolayers and LUV. Additionally, it can not be disregarded that probable coexisting phase domains might be enriched in PA (Vequi-Suplicy *et al.* 2010), leading to locally enhanced membrane surface negative charge and hence $StII_{1-30}$ activity.

Studies with GUV have proven to be a useful tool for following the mechanism of action of several bioactive molecules on lipid membranes. In our case, the effect of the peptides upon membrane causes a membrane optical contrast loss due to changes in its permeability. A detergent-like mechanism cannot be invoked to explain the phase contrast loss (Sudbrack *et al.* 2011) since both peptides seem to form relatively stable pores into GUV albeit at different concentrations (figure 4). Furthermore, as for $StII_{1-30}$, we had previously demonstrated its ability to form pores of around 1 nm of radius in erythrocytes (Casallanovo *et al.* 2006). It is worth mentioning that observations with GUV represent the first experimental evidence that $StII_{1-30}$ as well as $StI_{1-31}$ cause membrane injury by stable pore formation in liposomes.

In summary, the results showed in the current work demonstrates the relative contribution of hydrophobic and electrostatic forces as well as lipid heterogeneity to the differential activity of $StI_{1-31}$ and $StII_{1-30}$. Replacement of $Ala^1$ and $Ala^8$ in $StII_{1-30}$ by $Glu^2$ and $Asp^9$ and an extra $Ser^1$ turns $StI_{1-31}$'s 1–10 sequence less hydrophobic than $StII_{1-30}$, characterized by an uninterrupted hydrophobic segment. These features could be correlated with the higher activity of $StII_{1-30}$ by facilitating peptide partition and a deeper insertion of its N-terminus into membrane. The membranotropic action of $StII_{1-30}$ and $StI_{1-31}$ can be explained in terms of the balance of hydrophobic and electrostatic properties. Additionally, membrane heterogeneity plays an important role in binding and pore formation. Overall, this study suggests that the different activity of sticholysins could be due to a different penetration of their N-termini into the lipid bilayer governed by the balance of hydrophobic and hydrophilic properties.

## Acknowledgements

The authors thank Ms Frieda Aina Amapindi for her careful revision of the manuscript. This work was partly supported by CAPES-MES and CNPq-MES (Brazil-Cuba) collaboration projects. EMC, RI and SS are CNPq research fellows. UR is a grantee from IFS (4616), Sweden; TPS is a recipient from FAPESP fellowship.

## References

Álvarez C, Casallanovo F, Shida CS, Nogueira LV, Martínez D, Tejuca M, Pazos IF, Lanio ME, *et al.* 2003 Binding of sea anemone pore-forming toxins sticholysins I and II to interfaces-Modulation of conformation and activity, and lipid-protein interaction. *Chem. Phys. Lipids* **122** 97–105

Álvarez C, Mancheño JM, Martínez D, Tejuca M, Pazos F and Lanio ME 2009 Sticholysins, two pore-forming toxins produced by the Caribbean Sea anemone *Stichodactyla helianthus*: Their interaction with membranes. *Toxicon* **3457** 1–14

Anderluh G and Maček P 2002 Cytolitic peptide and protein toxins from sea anemones (Anthozoa: Actinaria). *Toxicon* **40** 111–124

Angelova M and Dimitrov D 1986 Liposome electroformation. *Faraday Disc. Chem. Soc.* **81** 303 – 311

Atherton E and Sheppard RC 1988 *Solid Phase peptide synthesis: A practical approach* (Oxford University Press)

Barlič A, Gutiérrez-Aguirre I, Caaveiro JM, Cruz A, Ruiz-Argüello MB, Pérez-Gil J and González-Mañas JM 2004 Lipid phase coexistence favors membrane insertion of Equinatoxin-II, a pore-forming toxin from *Actinia equina*. *J. Biol. Chem.* **279** 34209–34216

Belmonte G, Pederzolli C, Maček P and Menestrina G 1993 Pore formation by the sea anemone cytolysin equinatoxin II in red blood cells and model lipid membranes. *J. Membr. Biol.* **131** 11–22

Blondelle SE, Lohner K and Aguilar MI 1999 Lipid-induced conformation and lipid binding properties of cytolytic and antimicrobial peptides: determination and biological specifity. *Biochim. Biophys. Acta* **1462** 89–108

Brockman H 1999 Lipid monolayers: why use half a membrane to characterize protein-membrane interactions? *Curr. Opin. Struct. Biol.* **9** 438–443

Buck M 1998 Trifluoroethanol and colleagues: cosolvents come of age. Recent studies with peptides and proteins. *Q. Rev. Biophys.* **31** 297–355

Caaveiro JM, Echabe I, Gutierrez-Aguirre I, Nieva JL, Arrondo JL R and Gonzales-Mañas JM 2001 Differential interaction of equinatoxin II with model membranes in response to lipid composition. *Biophys. J.* **80** 1343–1353

Casallanovo F, de Oliveira FJF, de Souza FC, Ros U, Martínez Y, Pentón D, Tejuca M, Martínez D, Pazos F, Pretinhes TA, Spisni A, Cilli EM, Lanio ME, Álvarez C and Schreier S 2006 Model peptides mimic structure and function of the N-terminus of the pore-forming toxin Sticholysin II. *Biopolymers* **84** 169–180

Castrillo I, Alegre-Cebollada JG, Martínez del Pozo A, Gavilanes J, Santoro J and Bruix M 2009 1H, 13C, and 15N NMR assignments of the actinoporin Sticholysin I. *Biomol NMR Assign.* **3** 5–7

Chen RF and Knutson JR 1988 Mechanism of fluorescence concentration quenching of carboxyfluorescein in liposomes: energy transfer to non-fluorescent dimers. *Anal. Biochem.***172** 61–77

Cilli EM, Pigossi FT, Crusca E, Ros U, Martínez D, Lanio ME, Álvarez C and Schreier S 2007 Correlation between differences in amino-terminal sequences and different hemolytic activity of sticholysins. *Toxicon* **50** 1201–1204

Dalla Serra M, Fagiuoli G, Nordera P, Bernhart I, Della Volpe C, Di Giorgio D, Ballio A and Menestrina G 1999 The interaction of lipodepsipeptide toxins from *Pseudomonas syringae pv. syringae* with biological and model membranes: a comparison of syringotoxin, syringomycin and syringopeptins. *Mol. Plant - Microbe Interact.* **12** 391– 400

Eisenberg D, Weiss RM and Terwilliger TC 1984 The hydrophobic moment detects periodicity in protein hydrophobicity *Proc. Natl. Acad. Sci. USA* **81** 140–144

Huerta V, Morera V, Guanche Y, Chinea G, González LJ, Betancourt L, Martínez D, Álvarez C, *et al.* 2001 Primary structure of two cytolysin isoforms from *Stichodactyla helianthus* differing in their hemolytic activity. *Toxicon* **39** 1253–1256

Kem WR 1988 *Sea anemone Toxins: structure and action. The biology of the nematocyst* (New York: Academic Press)

Langner M and Kubica K 1999 The electrostatics of lipid surfaces. *Chem. Phys. Lipids* **101** 3–35

Lanio ME, Morera V, Álvarez C, Tejuca M, Gómez T, Pazos F, Besada V, Martínez M, Huerta V, Padrón G and Chávez MA 2001 Purification and characterization of two hemolysins from *Stichodactyla helianthus*. *Toxicon* **39** 187–194

Malovrh P, Barlič A, Podlesek Z, Maček P, Menestrina G and Anderluh G 2003 A novel mechanism of pore formation: Membrane penetration by the N-terminal amphipathic region of Equinatoxin. *J. Biol. Chem.* **278** 22678–22685

Mancheño JM, Martin-Benito J, Martínez-Ripoll M, Gavilanes JG and Hermoso JA 2003 Sticholysin II actinoporins revel insights into the mechanism of membrane pore formation. *Structure* **11** 1319–1328

Martínez D, Otero A, Álvarez C, Pazos F, Tejuca, M, Lanio ME, Gutiérrez-Aguirre I, Barlič A, *et al.* 2007 Effect of sphingomyelin and cholesterol in the interaction of St II with lipidic interfaces. *Toxicon* **49** 68–81

Martínez D, Soto C, Casallanovo F, Pazos F, Álvarez C, Lanio ME, Casallanovo F, Schreier S, *et al.* 2001 Properties of St I y St II, two isotoxins isolated from *Stichodactyla helianthus*: A comparison. *Toxicon* **39** 1547–1560

Op den Kamp JAF 1979 Lipid asymmetry in membranes. *Annu. Rev. Biochem.* **48** 47–71

Phillips MC, Graham DE and Hauser H 1975 Lateral compressibility and penetration into phospholipid monolayers and bilayer membranes. *Nature (London)* **254** 154–156

Pokorny A and Almeida PFF 2005 Permeabilization of raft-containing lipid vesicles by lysin: a mechanism for cell sensitivity to cytotoxic peptides. *Biochemistry* **44** 9538–9544.

Rouser G, Fkeischer S and Yamamoto A 1970 Two dimensional thin layer chromatographic separation of polar lipids and determination of phospholipids by phosphorus analysis of spots. *Lipids* **5** 494–496

Sackmann E 1995 Biological membranes architecture and function; in *Handbook of biological physics* (eds) R Lipowsky and E Sackmann (Amsterdam: Elsevier) pp 1–62

Simons K and Vaz WL 2004 Model systems, lipid rafts, and cell membranes. *Annu. Rev. Biophys. Biomol. Struct.* **33** 269–295

Sudbrack TP, Archilla NL, Itri R and Riske KA 2011 Observing the solubilization of lipid bilayers by detergents with optical microscopy of GUVs. *J. Phys. Chem. B* **115** 269–277

Tejuca M, Dalla Serra M, Ferreras M, Lanio ME and Menestrina G 1996 Mechanism of membrane permeabilization by sticholysin I, a cytolysin isolated from the venom of the sea anemone *Stichodactyla helianthus. Biochemistry* **35** 14947–14957

Tejuca M, Dalla Serra M, Potrich C, Álvarez C and Menestrina G 2001 Sizing the radius of the pore formed in erytrocytes and lipid vesicles by the toxin *sticholysin I* from the sea anemone *Stichodactyla helianthus. J. Membr. Biol*. **183** 125–135

Tossi A, Sandri L and Giangaspero A 2000 Amphipathic, alpha-helical antimicrobial peptides. *Biopolymers* **47** 465–477

Veatch SL and Keller SL 2002 Organization in lipid membranes containing cholesterol. *Phys. Rev. Lett.* **89** 268101

Vequi-Suplicy CC, Riske KA, Knorr RL and Dimova R 2010 Vesicles with charged domains. *Biochim. Biophys. Acta* **1798** 1338–1347

Yeaman MR and Yount NY 2003 Mechanisms of antimicrobial peptide action and resistance. *Pharmacol. Rev.* **55** 27–55

*MS received 07 June 2011; accepted 17 August 2011*

*e*Publication: 29 October 2011

Corresponding editor: AMIT CHATTOPADHYAY